EPJ Web of Conferences **302**, 13011 (2024) https://doi.org/10.1051/epjconf/202430213011
SNA + MC 2024

Benchmarking of the SPERT-III E-core experiment with the Monte Carlo codes TRIPOLI-4®, TRIPOLI-5® and OpenMC

Antoine Dervaux[1], *Shai* Kinast[2], *Matthieu* Lemaire[1], *Vincenzo* Di Blasi[1], *Coline* Larmier[1], *Davide* Mancusi[1] and *Andrea* Zoia[1]

[1]Université Paris-Saclay, CEA, Service d'Études des Réacteurs et de Mathématiques Appliquées, 91191, Gif-sur-Yvette, France.
[2]Department of Physics, Nuclear Research Center Negev, Beer Sheva 8410501.

Abstract. This paper presents a code-to-code verification of the SPERT-III reactor in its E-core configuration using the Monte Carlo codes TRIPOLI-4®, TRIPOLI-5® and OpenMC. A SPERT-III E-core model was originally developed for the Monte Carlo code TRIPOLI-4® and will be the baseline of our analysis The simulation results obtained for the main reactor physics parameters (neutron effective multiplication factor, rod worth, reactivity coefficients and kinetics parameters) with TRIPOLI-4®and OpenMC using different nuclear data libraries are compared and analyzed. Additional verifications are carried out with the next-generation Monte Carlo code TRIPOLI-5®, which is currently under development by CEA and IRSN (France). This paper summarizes a joint study that was conducted within an international research collaboration between CEA Paris-Saclay (France) and the Nuclear Research Center Negev (NRCN, Israel), and is a stepping stone towards future multi-physics simulations exploring the SPERT-III reactor power excursions, including thermal-hydraulics feedback.

1 Introduction

The Special Power Excursion Reactor Test III (SPERT-III) was a pressurized-water research reactor operated in the United States in the 1960s. The main objective of SPERT-III was to analyze the kinetic behavior of nuclear reactors with the aim of evaluating the safety and thermo-mechanical constraints of structural materials. The experimental measurements available for the E-core configuration of SPERT-III have attracted a considerable interest from the nuclear reactor physics community in view of the possibility of validating neutronics and thermal–hydraulics codes in both steady-state and transient conditions.
The present work is the first step of an ongoing international research collaboration between CEA Paris-Saclay, France, and the Nuclear Research Center Negev (NRCN), Israel, aiming at exploring the transient behavior of the SPERT-III reactor with multi-physics calculation schemes. The starting point of this work is a SPERT-III E-core reactor model initially conceived for the Monte Carlo code TRIPOLI-4® (developed at CEA) in 2016, using the ROOT geometry package [1]. A new constructive solid geometry (CSG) model of the SPERT-III E-core reactor is first developed for the OpenMC code based on the original

TRIPOLI-4® model. Then, a verification study of the new model is conducted with the Monte Carlo codes TRIPOLI-4® and OpenMC by comparing, for several configurations of the SPERT-III reactor, the results of static calculations (neutron effective multiplication factor, rod worth, Doppler and void coefficients and kinetic parameters) with the nuclear data libraries JEFF3.3 and ENDF/B-VIII.0. Additional verifications are carried out with the next-generation Monte Carlo code TRIPOLI-5®, which has been jointly developed by CEA and IRSN (France) since 2022, using both the same ROOT-based model originally developed for TRIPOLI-4® and a new CSG model developed using the AGORA native geometry engine of TRIPOLI-5®. The primary goal of this paper is to develop and verify a model of the SPERT-III reactor for the OpenMC code in the stationary regime. This model will be used for future code-to-code comparisons involving multi-physics transient studies of the SPERT-III reactor. A secondary goal is the verification of the stationary criticality calculations of the TRIPOLI-5® code using different geometry models.
This paper is structured as follows. In Section 2, we present the Monte Carlo neutron-transport codes and the nuclear data libraries used in this work. In Section 3, we provide the description of the key elements of the SPERT-III E-core models, whose reference technical specifications were retrieved from the original SPERT-III reports [2-7]. Finally, in Section 4, we describe and analyze the simulation results obtained with these codes. Section 5 presents the conclusions and the perspectives.

2 Monte Carlo codes and nuclear data libraries

2.1 TRIPOLI-4® and TRIPOLI-5® Monte Carlo codes

CEA has been developing the TRIPOLI (TRIdimensionnel POLYcinétique) family of codes since the 1960s. TRIPOLI-4® is the fourth generation and its development started in the 1990s [8]. This code uses continuous-energy nuclear data and arbitrary three-dimensional models for particle-transport applications in the fields of reactor physics, criticality-safety, radiation shielding and nuclear instrumentation. The original SPERT-III model conceived for TRIPOLI-4® in 2016 is described by means of the ROOT geometry package developed by CERN [9]. The version of TRIPOLI-4® used for the present work is TRIPOLI-4.12, released in 2022.
TRIPOLI-5® is a next-generation Monte Carlo code currently under joint development by CEA and IRSN [10, 11]. In the short term, its main focus is on multi-physics calculations at the core level, including stationary, depletion and kinetic regimes. In the long term, it is supposed to replace TRIPOLI-4® over a broader range of applications. An alpha version of TRIPOLI-5® was used for this work.

2.2 OpenMC Monte Carlo code

OpenMC is an open-source Monte Carlo code whose development started at the Massachusetts Institute of Technology (MIT), which is now the main contributor together with the Argonne National Laboratory (ANL) [12]. OpenMC is capable of performing fixed source and k-eigenvalue calculations on models built using either a constructive solid geometry (CSG) or computer-aided design (CAD) representation. The version of OpenMC used in this work is v0.14.1.

2.3 JEFF3.3 & ENDF/B-VIII.0 nuclear data libraries

The joint Evaluated Fission and Fusion (JEFF) nuclear data library is a collaboration between NEA (Nuclear Energy Agency) Data Bank participating countries. The JEFF library combines the efforts of different working groups to produce sets of evaluated nuclear data, for fission and fusion applications [13]. In 2022, a new version of the JEFF data library, named JEFF-3.3, was released with relevant updates in the neutron reaction, thermal neutron scattering and covariance sub-libraries.
The Evaluated Nuclear Data File (ENDF) library project is managed by the Cross Section Evaluation Working Group (CSEWG), beginning in 1966, and has produced seven major and numerous minor library releases since. The major version ENDF/B-VIII.0 was released in 2018 [14].
In this work we will rely on both the JEFF-3.3 and the ENDF/B-VIII.0 libraries, in order to evaluate the impact of the choice of the nuclear data on the obtained results.

3 Description of the SPERT-III E-core

SPERT-III is a pressurized light-water-moderated reactor with 4.8% enriched UO_2 fuel rods. The standard E-core configuration of the SPERT-III reactor contains 60 assemblies, including 48 fuel assemblies with 25 (5 by 5) pin cells, four assemblies with 16 (4 by 4) pin cells and eight control rods with fuel followers. A multi-layered stainless-steel vessel surrounds the core. A transient cruciform boron-steel rod is located at the center of the core: the rapid ejection of this rod is used to insert the necessary reactivity to initiate the sought power excursion. The general view and a radial view of SPERT-III are shown in **Fig. 1.** The TRIPOLI-4® model was described in Ref. [1], to which we refer the reader: in the following, we will mainly focus on specific points of implementation details in relation to choices to be made for the new OpenMC model.
The SPERT-III configuration was implemented in OpenMC using the python-based geometry description module of OpenMC. A geometry-checking tool developed by CEA was used to verify and enforce the consistency between the original ROOT-based geometry for TRIPOLI-4® and the new python-based CSG geometry for OpenMC.

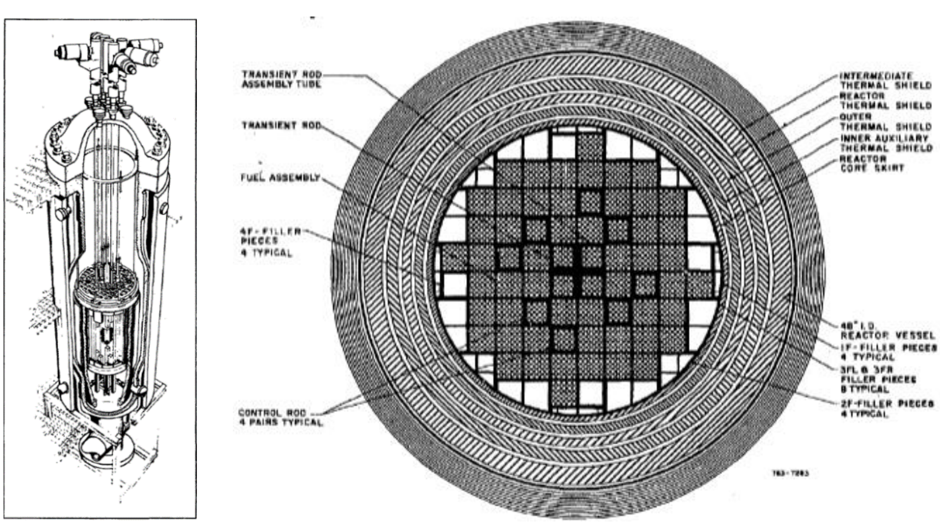

Fig. 1. General view of the SPERT-III reactor (left) and radial view (right) [2].

3.1 Fuel assemblies

The UO_2 fuel (at 4.8% enrichment) comes in 0.42-inch outer diameter pellets contained in SS348 stainless steel tubes, with a 0.003-inch radial gas gap between the pellets and the inner wall of the fuel cladding. In order to preserve the symmetry of the lattice, the core is composed of two types of fuel assemblies, namely 5x5 elements and 4x4 elements. The standard 5x5 fuel elements contain 25 fuel rods arranged in a regular 5x5 array with a pitch of 0.585 inch. For cooling purposes, water circulation is enabled through holes in the SS348 assembly boxes of the 5x5 fuel assemblies (see **Fig. 2**). The precise details of the geometry of the assembly box holes are not known. In the TRIPOLI-4® model developed in [1], the water contained in the holes and the stainless steel box have been homogenized based on the total volume of the holes. We have thus chosen to keep this approximation for the OpenMC model. The 4x4 fuel assemblies are similar to the 5x5 assemblies, sharing the same fuel rods and the same pitch. The 4x4 fuel assemblies are only located around the transient rod and in the fuel follower part of control rods. Finally, 348SS stainless-steel plugs complete the fuel rods between the active core and the grids.

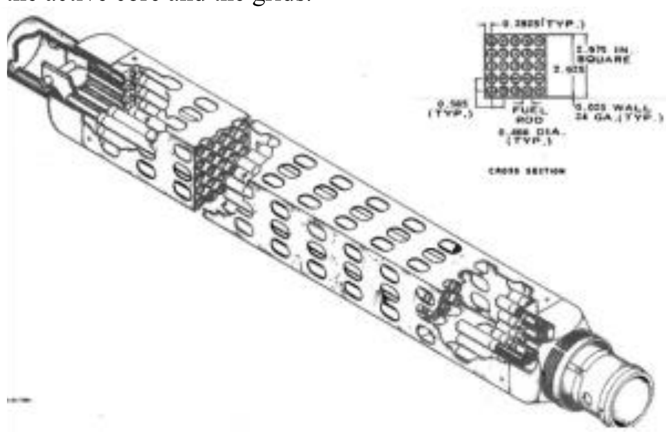

Fig. 2. General view of a fuel assembly of the SPERT-III reactor [2].

3.2 Control rods

Four pairs of control rods of the SPERT-III reactor are inserted from the top of the reactor and have the following specifications:

- The fuel follower, at the bottom of the control rod, consists in 4 by 4 fuel rod assemblies protected by a 0.475-cm-side square zircaloy guide tube.
- The absorber part, at the top of the control rod, consists in moderator surrounded by 0.472-cm 304 borated stainless-steel square casing at 1.35% boron enrichment in the steel, which is itself protected by a 0.475-cm square zircaloy guide tube.
- The flux suppressor, at the junction between the fuel follower and the absorber part. The flux suppressor is itself divided in several parts, from top to bottom:
    1. an absorber grid surrounded by stainless-steel with 1.35% boron tube;
    2. an absorber grid with moderator in-between;
    3. a stainless-steel plate with 3x3 moderator holes in-between;
    4. an absorber grid with stainless-steel rods in-between;
    5. an absorber grid with fuel rods in-between.

The geometry of the flux suppressor is shown in **Fig. 3**. The part labeled “A” corresponds to the absorber part of the control rod and the part labeled “B” is the fuel follower.

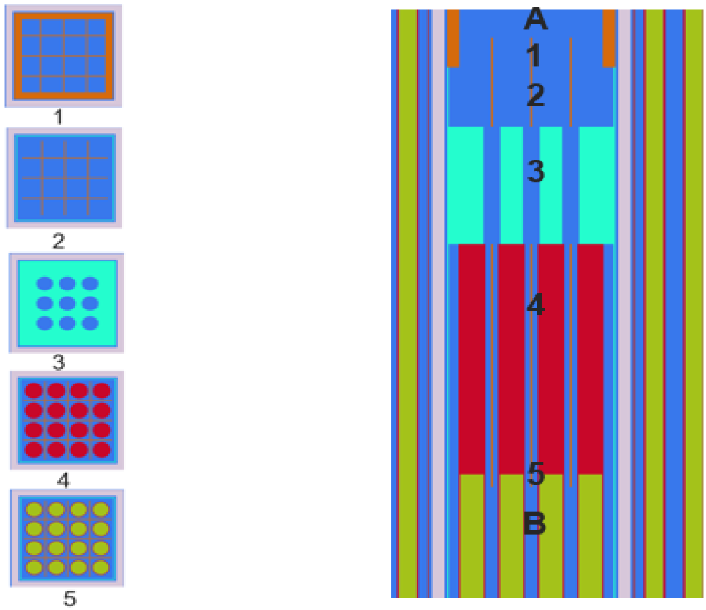

Fig. 3. Radial view of the different parts of the flux suppressor in OpenMC (left) and axial view of the flux suppressor in OpenMC (right).

3.3 Transient rod

The transient rod, which as a cruciform shape, is used to insert reactivity and initiate power excursions for experimental purposes. In normal operating conditions, the upper section of the transient rod (made of stainless steel) is in the core, whereas the lower section (made of 1.35% borated steel) is outside the core. In order to respect the symmetry of the core, the four fuel elements located around the transient rod are of the 4x4 type (with the same kind of fuel rods and array pitch as for the 5x5 assemblies).
A guide tube made of Zircaloy-2 protects the transient rod and the four surrounding fuel elements. **Fig. *4*** represents the transient rod and a radial view of the reactor core model with the transient rod located in its center.

3.4 Top and bottom grids

Upper and lower 304L stainless steel grids support the fuel elements in the core. The lower grid has a thickness of 3 inches and has a diameter of 31.97 inches, with holes corresponding to fuel element locations and core fillers, plus a cruciform hole for the transient rod. The upper grid has a thickness of 7 inches and has a diameter of 42 inches, with holes for the fuel assemblies, the transient rod and the control rods. The holes at the top have a 0.444-inch radius, while the holes at the bottom have a 1.03-inch radius. The top grid has moderator above and around it, while the bottom grid has moderator only below it. The grids are shown in **Fig. 5.**

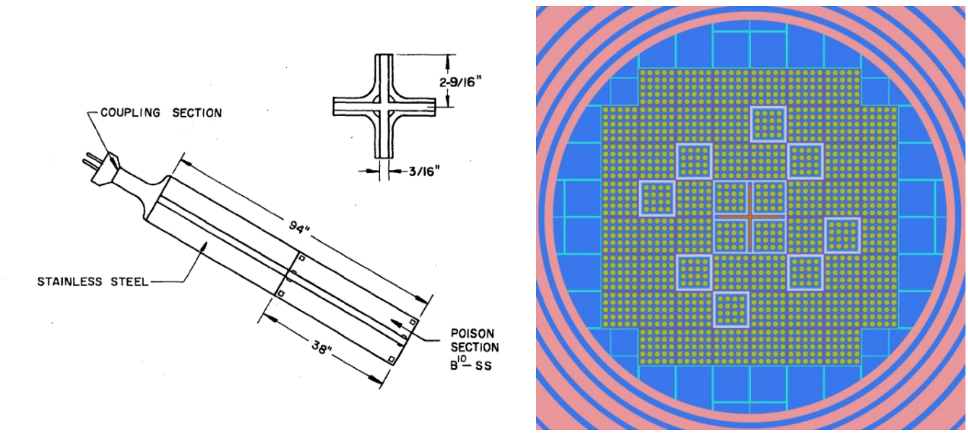

Fig. 4. General view of the transient rod of the SPERT-III reactor (left) [2] and the radial view of the reactor model developed for OpenMC with the transient cross in the middle (right).

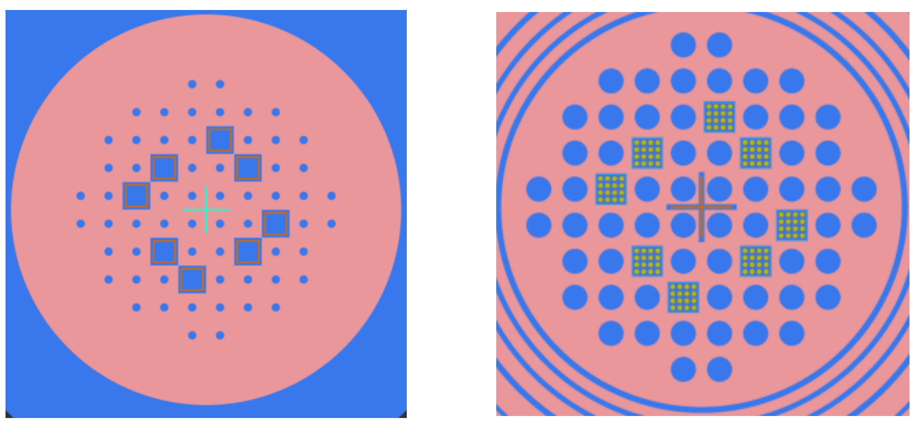

Fig. 5. Radial view of the top grid of the SPERT-III reactor (left) and radial view of the bottom grid (right) corresponding to the reactor model developed for OpenMC.

4 Code-to-code verification between TRIPOLI-4®, TRIPOLI-5® and OpenMC

In this section we present the computed reactor parameters obtained using TRIPOLI-4®, TRIPOLI-5® and OpenMC and discuss the results in comparison with experimental reactor data measured in 1967 [6, 7]. Calculations with TRIPOLI-5® were run twice: first with a ROOT geometry of the SPERT-III reactor, identical to the ROOT geometry model used for TRIPOLI-4® calculations; then with the newly developed AGORA native geometry engine of TRIPOLI-5®.
For all the codes, simulations are carried out with the ENDF/B-VIII.0 and JEFF3.3 nuclear data libraries with $S(\alpha,\beta)$ thermal scattering data for hydrogen in water. Special care is applied to enforce the same physical neutron-transport models in the three codes, in order for the code-to-code verification to be fair. The Doppler broadening of the elastic scattering kernel

is taken into account by applying the DBRC (Doppler Broadening Rejection Correction) model available in TRIPOLI-4®, TRIPOLI-5® and OpenMC on every nuclide, up to a cutoff energy of 1 keV. The calculations are run using 15000 batches and 15000 neutrons per batch to obtain an uncertainty on the effective multiplication factor at 1σ (67% confidence interval) of about 10 pcm. The Shannon entropy was estimated with TRIPOLI-4® to assess the stationarity of the fission sources: based on this analysis (and on previous numerical investigations carried out in Ref. [1]), the first 300 batches are discarded before beginning the tallies. Probability tables, whose impact has been previously evaluated as practically negligible [1], are not used. A critical configuration of the SPERT-III reactor is of special interest for this investigation, namely the cold zero power (CZP) condition. The control rods are placed at 14.6 in from the bottom of the active fuel zone with respect to the top of the flux suppressor (transition between part A and region 1 in **Fig. 3**), and the top of the poison part of the transient rod is placed at 0 in from the bottom of the active fuel zone (outside the core). The temperature of the CZP configuration is set at 70°F. In the rest of this section, uncertainties are given at 1σ.

4.1 Reactivity calculations

Reactivities computed with the three codes for the critical CZP configuration are presented in **Table 1.** The results are close to the critical state, as expected, and the codes are in good agreement with each other, thus providing confidence in the correctness and consistency of the implemented reactor models.

Table 1. Reactivity results obtained for CZP with the three codes.

Code	CZP Keff	Difference from TRIPOLI-4® (pcm)
ENDF/B-VIII.0		
TRIPOLI-4.12®	$1.00029 \pm 7 \times 10^{-5}$	-
TRIPOLI-5® + ROOT	$0.99971 \pm 9 \times 10^{-5}$	58 ± 11
TRIPOLI-5® + AGORA	$1.00018 \pm 10 \times 10^{-5}$	11 ± 12
OpenMC	$0.99922 \pm 8 \times 10^{-5}$	107 ± 11
JEFF3.3		
TRIPOLI-4.12®	$1.00289 \pm 7 \times 10^{-5}$	-
TRIPOLI-5® + ROOT	$1.00262 \pm 9 \times 10^{-5}$	27 ± 11
TRIPOLI-5® + AGORA	$1.00312 \pm 10 \times 10^{-5}$	-23 ± 12
OpenMC	$1.00235 \pm 8 \times 10^{-5}$	54 ± 11

For reference, in the investigation carried out in Ref. [1], the CZP configuration yielded a Keff of $1.00139 \pm 11 \times 10^{-5}$ using TRIPOLI-4.10® and JEFF-3.1.1 and Keff of $1.00163 \pm 11 \times 10^{-5}$ using TRIPOLI-4.10® and ENDF/B-VII.0.

4.2 Effective delayed neutron fraction β_{eff} and mean neutron generation time Λ_{eff}

The kinetic parameters (effective delayed neutron fraction β_{eff} and neutron generation time Λ_{eff}) are computed with TRIPOLI-4® using the Iterated Fission Probability (IFP) method [15]. For OpenMC and TRIPOLI-5®, as the reference IFP method is not available, two methods described in [16], namely the “Keff method” and the “production method”, are applied to determine an approximation of β_{eff}.

The "Keff method" consists in calculating the Keff (effective neutron multiplication factor) in a given configuration and then calculating a "Kp value" (prompt K) corresponding to the Keff without delayed neutrons. Then, the effective delayed neutron fraction is approximated as

$$\beta_{\text{eff}} \simeq 1 - \frac{K_p}{K_{\text{eff}}} \qquad (1)$$

The "Production method" consists in calculating the total fission production P_T and the prompt fission production P_p. Then, the effective delayed neutron fraction is approximated as

$$\beta_{\text{eff}} \simeq 1 - \frac{P_p}{P_T} \qquad (2)$$

The total fission production and the prompt fission production contributions are easily obtained in both TRIPOLI-4® and OpenMC using reaction rate tallies.
Table 2 shows β_{eff} results obtained with TRIPOLI-4® and OpenMC, using the ENDF/B-VIII.0 and JEFF3.3 data. The results are close to each other and in good agreement with the reference value obtained with the IFP method. In the next sections, the value of 1 dollar (1 $) of reactivity for the normalization of the reactivity worth is set equal to the computed IFP value, that is 1 $ = 748 pcm for all codes for the ENDF/B-VIII.0 library and 1 $ = 771 pcm for all codes for the JEFF3.3 library. As for the mean neutron generation time, the Λ_{eff} value was determined to be 17.23 ± 0.05 µs with TRIPOLI-4® and was not computed with OpenMC and TRIPOLI-5®.

Table 2. Values of β_{eff} computed with different methods with TRIPOLI-4®, OpenMC and TRIPOLI-5®.

Method	TRIPOLI-4.12® (pcm)	OpenMC (pcm)	TRIPOLI-5® + ROOT (pcm)	TRIPOLI-5® + AGORA (pcm)
ENDF/B-VIII.0				
IFP	748 ± 3	N/A	N/A	N/A
Keff method	773 ± 6	731 ± 9	772 ± 12	784 ± 12
Production method	754 ± 9	710 ± 12	N/A	N/A
JEFF3.3				
IFP	771 ± 2	N/A	N/A	N/A
Keff method	775 ± 11	735 ± 12	N/A	N/A
Production method	776 ± 6	755 ± 12	N/A	N/A

Additionally, the kinetics parameters obtained in 2016 in Ref. [1] with TRIPOLI-4.10® and JEFF-3.1.1 are : β_{eff} = 761 ± 4.6 pcm and Λ_{eff} = 17.3 ± 0.06 µs. With TRIPOLI-4.10® and ENDF/B-VII.0, they are : β_{eff} = 734 ± 1.6 pcm and Λ_{eff} = 18.8 ± 0.007 µs, which is in good agreement with the results above.

4.3 Control rod worth

To determine the reactivity worth, control rods are displaced by 5 cm steps starting from the critical configuration at CZP. For each step, a criticality calculation is run, the Keff is determined and the differential and the integral rod worth are deduced. The differential rod worth is defined as the difference between the reactivity at step i and the one at step i+1. The integral rod worth is calculated by determining the reactivity brought by the rods from the point of reference (14.6 inches = 37.083 cm) to the i-th step. **Fig. *6*** shows the differential rod worth as well as the integral rod worth compared to the fitted experimental results. A good agreement is observed between the three codes, with an overall satisfactory consistency with the fitted experimental data.

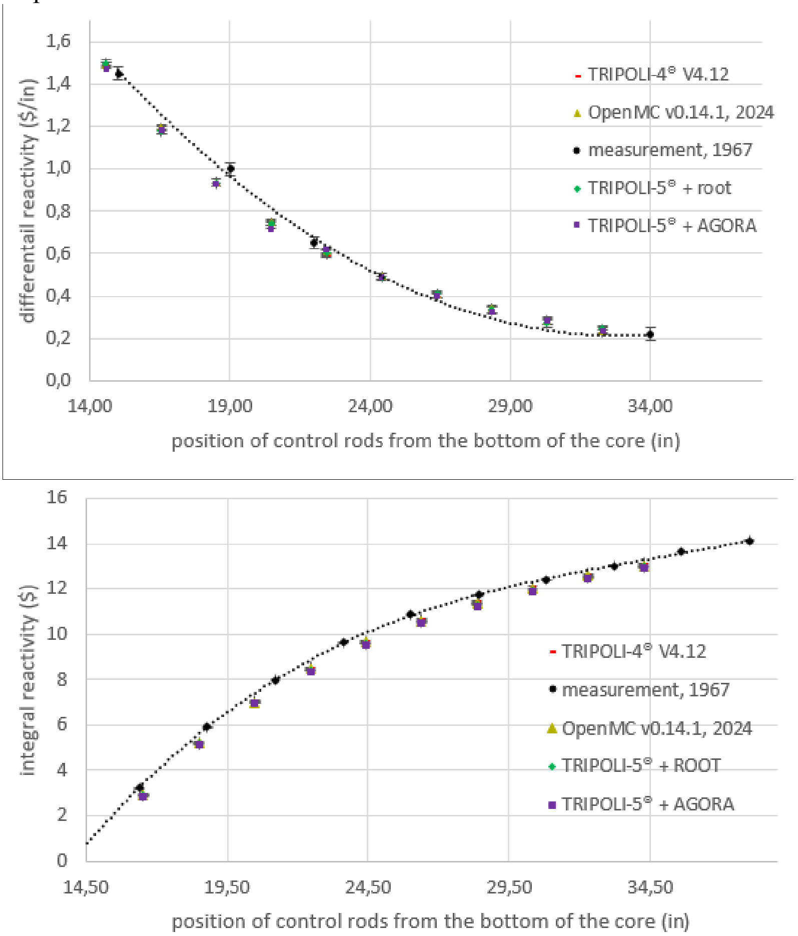

Fig. 6. Differential control rod worth (top), and integral control rod worth (bottom) for TRIPOLI-4®, TRIPOLI-5®, OpenMC and measurements of 1967 for the CZP configuration with ENDF/B-VIII.0.

4.4 Transient rod worth

To determine the transient rod worth, the control rods are maintained at the "critical" position of the CZP configuration and the transient rod is inserted from 6 cm to 20 cm, by 2-cm steps. At each step, a criticality calculation is run, the corresponding Keff is estimated, and the integral rod worth is consequently deduced. In **Fig. 7** we compare the integral transient rod worth obtained with TRIPOLI-4.12®, OpenMC and TRIPOLI-5®, and the fitted experimental measurements of 1967 [6, 7]. Furthermore, the total anti-reactivity worth of the transient rod is reported in **Table 3**.

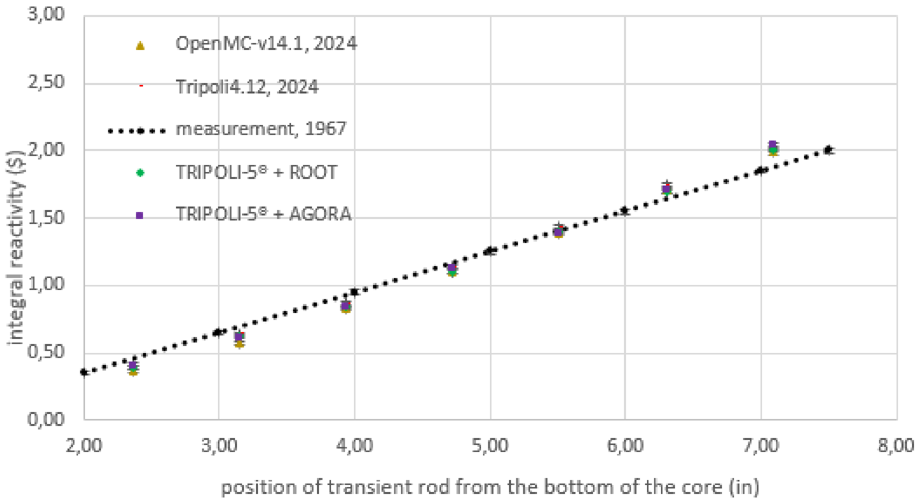

Fig. 7. Integral transient rod worth for TRIPOLI-4®, TRIPOLI-5®, OpenMC and measurements [6, 7] for the CZP configuration.

Table 3. Total anti-reactivity of the transient rod for TRIPOLI-4®, TRIPOLI-5®, OpenMC and measurements of 1966 for the CZP configuration.

	Measurement, 1966 [6, 7]	TRIPOLI-4.12®	OpenMC	TRIPOLI-5® + ROOT	TRIPOLI-5® + AGORA	Nuclear data
Total anti-reactivity ($)	4.6	4.33 ± 0.02	4.31 ± 0.01	4.33 ± 0.02	4.36 ± 0.02	JEFF3.3
		4.49 ± 0.02	4.48 ± 0.01	4.49 ± 0.02	4.48 ± 0.02	ENDF/B-VIII.0

A slight discrepancy between the calculations and the measurements is observed, which can be partially explained by the approximations on the model of the transient rod (a few geometrical details were not precisely given in the original documents and had to be guessed). Nevertheless, the computed results are close to each other and within 10% of the measured values. Additionally, the total anti-reactivity obtained in 2016 in Ref. [1] with TRIPOLI-4.10® and JEFF-3.1.1 equals 4.42 ± 0.03 $, which is in good agreement with the results above.

4.5 Temperature defect

The changes in system reactivity due to variations in the water moderator have been experimentally determined in [6, 7] under steady state conditions. The isothermal temperature coefficient has been measured by uniformly varying the temperature of all the components of the reactor between approximately 70 °F and 574 °F by intervals of 50 °F at each step. The integral temperature defect curve is displayed in **Fig. 8**, together with the corresponding results obtained by TRIPOLI-4® and OpenMC by modifying the temperature of reactor components and re-computing the water density accordingly. Calculations were run only with ENDF/B-VIII.0 with TRIPOLI-4® and OpenMC as the set of needed temperatures is not yet available with TRIPOLI-5®.

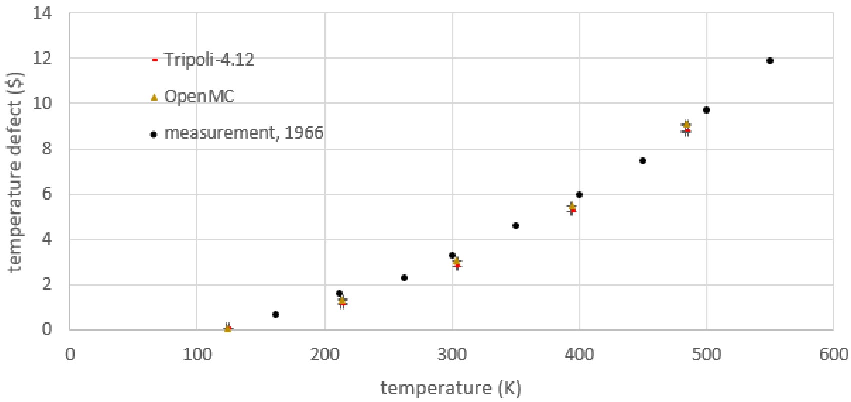

Fig. 8. Integral temperature defect for TRIPOLI-4®, OpenMC and the measurements of 1966 [6, 7] with ENDF/B-VIII.0.

4.6 Void and Doppler coefficient

In references [6, 7], the void coefficient was experimentally measured by inserting aluminum wires in the moderator and determining the corresponding change in system reactivity. In this work, this coefficient was estimated by modifying the density of the moderator by 1%:

$$\alpha_v = \frac{K_{\text{eff}}(+1\%) - K_{\text{eff}}(-1\%)}{2(\%)} \quad (3)$$

The Doppler coefficient was determined for all the codes by modifying the temperature of the fuel rods:

$$\alpha_m = \frac{K_{\text{eff}}(T_1) - K_{\text{eff}}(T_2)}{T_2 - T_1} \quad (4)$$

T_1 being 294 K and T_2 being 274 K for TRIPOLI-4® and OpenMC. For TRIPOLI-5®, T_2 is 250 K with ENDF/B-VIII.0 and 600 K with JEFF3.3. **Table 4** shows the results obtained for the void and Doppler coefficients. For comparison, in Ref. [1], the void coefficient obtained with TRIPOLI-4.10® and JEFF3.1.1 equals -0.44 ± 0.02 $/%-void and the Doppler coefficient is -0.28 ± 0.02 ¢/°F. Computed results are close to each other, with a good agreement between the codes.

5 Conclusions and perspectives

An OpenMC model of the SPERT-III reactor in its E-core configuration was developed based on an existing ROOT geometry model previously developed for TRIPOLI-4®. A good agreement is observed between TRIPOLI-4® and OpenMC for the reactivities at CZP, the kinetic parameters, the control rod worth and the reactivity coefficients, using the JEFF-3.3 and ENDF/B-VIII.0 libraries. These results suggest that the essential features of the E-core have been captured in the proposed Monte Carlo model for OpenMC. A good agreement is also observed with the values computed with the TRIPOLI-5® code, currently under development, for which calculations have been run using alternatively the same ROOT-based geometry model as for TRIPOLI-4® and a newly developed model based on the AGORA CSG native geometry engine of TRIPOLI-5®. For all tested quantities, the estimated results are consistent with the experimental measurements.

This work paves the way for future investigations of multi-physics transients of the SPERT-III reactor.

Table 4. Void coefficient (left) and Doppler coefficient (right) obtained with different codes.

	Void coefficient ($/%-void)	Doppler coefficient (¢/°F)
ENDF/B-VIII.0		
measurement	-0.5 ± 0.025	N/A
TRIPOLI-4.12®	-0.42 ± 0.05	-0.292 ± 0.02
TRIPOLI-5® + ROOT	-0.40 ± 0.05	-0.253 ± 0.02
TRIPOLI-5® + AGORA	-0.38 ± 0.06	-0.283 ± 0.02
OpenMC	-0.39 ± 0.05	-0.283 ± 0.02
JEFF3.3		
measurement	-0.5 ± 0.025	N/A
TRIPOLI-4.12®	-0.38 ± 0.05	-0.221 ± 0.02
TRIPOLI-5® + ROOT	-0.38 ± 0.05	-0.190 ± 0.02
TRIPOLI-5® + AGORA	-0.39 ± 0.05	-0.184 ± 0.02
OpenMC	-0.38 ± 0.04	-0.226 ± 0.02

References

1. A. Zoia, E. Brun, Reactor physics analysis of the SPERT III E-core with TRIPOLI-4®, Annals of Nuclear Energy, volume 90, Pages 71-82 (2016)
2. J. Dugone, SPERT-III reactor facility: E-CORE revision, IDO-17036 (1965)
3. Heffner et al., SPERT-III reactor facility, IDO-16721. (1961)
4. Houghtaling et al., Addendum to the SPERT-III hazards summary report. Low- enrichment oxide core, IDO-17003 (1965)
5. McCardell et al., Reactivity accident test results and analyses for the SPERT-III E-CORE - A small oxide-fueled, pressurized-water reactor, IDO-17281. (1969)
6. Taxelius et al., Quarterly technical report SPERT project, IDO-17228 (1967)
7. Taxelius et al., Quarterly technical report SPERT project, IDO-17245 (1967)
8. E. Brun et al., Tripoli-4®, CEA, EDF and AREVA reference Monte Carlo code, Annals of Nuclear Energy no 82, Pages 151-160. (2015)
9. R Brun, A Gheata, M Gheata Nuclear Instruments and Methods in Physics Research Section A
10. C. Larmier et al., Preliminary code-to-code comparisons for the implementation of neutron and photon physics in the new Monte Carlo transport code TRIPOLI-5. International Conference on Mathematics and Computational Methods Applied to Nuclear Science and engineering (2023)
11. Mancusi D et al., Overview of TRIPOLI-5, a Monte Carlo code for HPC, submitted to EPJ Nucl. Sci. Technol. (2024)
12. Paul K. Romano et al., The OpenMC Monte Carlo particle transport, Annals of Nuclear Energy volume 51, Pages 274-281 (2013)
13. Plompen et al., The joint evaluated fission and fusion nuclear data library, JEFF-3.3. Eur. Phys. J. A 56, 181 (2020).
14. D. A. Brown, The 8th Major Release of the Nuclear Reaction Data Library with CIELO-project Cross Sections, New Standards and Thermal Scattering Data (2018)
15. G. Truchet et al., Computing adjoint-weighted kinetics parameters in Tripoli-4 by the Iterated Fission Probability method. Annals of Nuclear Energy, no 85, Pages 17-26 (2015)
16. C. Steven et al., Calculating the effective delayed neutron fraction using Monte Carlo techniques, PHYSOR, (2004)
17. R.C Wang et al., Validation of the U.S. NRC coupled code system TRITON/TRACE/PARCS Using the SPERT III, Nuclear Technology, volume 183 b (2013)